Target Tracking and Predictive Control Using Rfid for Mobile Robot based on Self Generated Polar Grids

Kajon Anuditaya[+,1], Kasemsak Uthaichana[+,2] and Boonsri Kaewkham-ai[+,3]

[+]Department of Electrical Engineering, Faculty of Engineering, Chiang Mai University, Chiang Mai, Thailand, 50200. Tel +66-53-944-140

[1]anuditaya@hotmail.com, [2]kasemsak@chiangmai.ac.th, [3]boonsri@eng.cmu.ac.th

Abstract. This paper presents a target tracking control of a wheeled mobile robot (WMR) using a passive RFID tag and a reader for navigation system. The task at the supervisory level is decomposed into the localization based on self-generated grids, and the trajectory planning using the model predictive control (MPC) strategy. In contrast to other work in literatures, only a single RFID tag is used to designate the target, while a single reader is attached to the WMR; and no other sensing hardware is required. During the localization step, the polar grids are self-generated via the intersection of the selected distances, and the angles from the WMR. Different distances and angles are achieved by the variation in the reader intensities and the heading positions, respectively. The localization error of the generated polar grids is naturally magnified as the target is farther away from the WMR. For the MPC strategy in this work, the WMR is estimated to complete the trajectory in two control windows, but only the first window of the planned control sequence is applied. At the end of the first control window, the target position is then re-estimated, and the process is repeated. The MPC allows the WMR to cope with the localization error, which is smaller when the target distance becomes nearer. The tradeoff between the WMR's traveling time duration to the target, and the tracking robustness is explored in this study. The obtained simulation results have shown that the MPC with conservative setting in the first control window is more robust to the localization error and disturbances.

Keywords: Wheeled Mobile Robot; passive RFID; Model Predictive Control; Localization.

1. IntroductionEquation Section 1

Many applications, such as in rescuing missions, wheel chairs for the handicapped, and in industrial inventory management, employ wheel mobile robots (WMR). The control problem of WMR at the supervisory level can be decomposed into the target localization, and the trajectory planning and local control. Many sensors are used for the target localization such as GPS, camera, sonar, ultrasonic, etc. The RFID based, popular as indoor sensors for target identification, has active tag options allowing for wider ranges for detection, but is unfortunately expensive. Passive tags are cheaper, but the target localization problem is not straightforward. To achieve high level of accuracy, usually massive number of tags are required. In fact, the level of error is inversely proportional to the square of the number of tags (n^2). In [1], fixed pattern of triangular grid orientation is shown more accurate than the square orientation counterpart. However, in previous researches [2-5], the tags are always fixed at predetermined locations, and the location information for each tag is stored onboard. This method is not suitable for mobile applications where the working platform often moves. The trajectory planning and the local control step uses the information from the localization scheme to navigate the WMR to the target. In [6-9], various fuzzy logic controls are created to move the WMR with the main idea based on simple sets of rules. In model based control, an objective function is optimized by the robot onboard [10]. The decision yields an optimal cost; however, the required computation is still extensive, and accurate mathematical model representation is also required.

In this work, instead of fixing many RFID tags at predetermined coordinates, only a single passive RFID tag is required for the target localization. The localization grid is generated by the intersection of the iso-intensity lines and the lines of angles with respect to the robot heading as illustrated in Fig. 1(a).

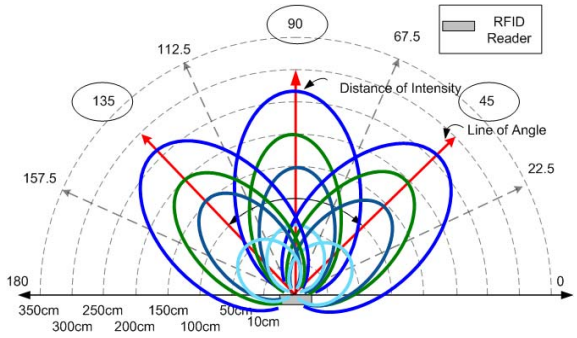

(a)

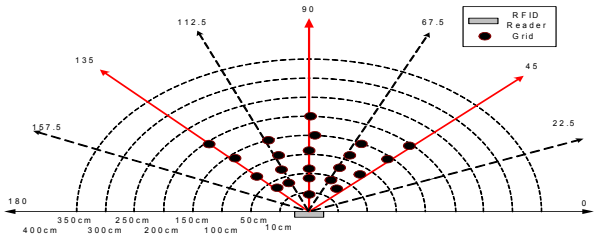

(b)

Fig. 1 (a) Idea of self-generated polar grids (b) Selected nominal grids

The accuracy level of the position from the localization step has the direct impact on the choice of the trajectory planning strategy. The adopted estimated position contains small error for the target close to WMR; however, the error becomes larger as the target is further away from the WMR's reader. This is directly resulted from the nature of the polar grids. The model predictive control (MPC) [11-13] has been known to deal with the plant modeling error and disturbances such as unknown road conditions. The trajectory is planned and the control sequence is computed based on the estimated position. However, only the first control window is executed. Then, the process is repeated. The choice of the local closed-loop controller, such as in [14], is then selected to propel the DC motors of the WMR at the prescribed profile.

The localization scheme is presented next section. Section 3 is the summary on the MPC and the performance index to be optimized. Section 4 presents the results. The conclusion is given last.

2. Localization via Self-Generated Grids Equation Section (Next)

To generate the polar coordinate using a single RFID tag for the target, the reader sends the RF signal with the intensity I_r of 3, 6, 9 and 12 dB. The transmission angle θ_r is also varied at 45, 90, and 135 degrees, where 90 degree is denoted the front of the WMR. For each target position, the reading result for the pair (I_r, θ_r) is found/not found, i.e., (1/0), by constructing the sequence of the reading, $\{s_i\}$, it can be used as the IDs to represent different target positions in the working space of the WMR. An example of the reading for all four intensity levels and three heading angles are depicted in Table 1.

Table 1. Examples of reading results for various positions

12dB			**9dB**			**6dB**			**3dB**		
45	90	135	45	90	135	45	90	135	45	90	135
1	1	1	1	1	1	1	1	1	0	1	0

However, the limitation of this localization method is found as follows. When two different target positions are in the same vicinity and the reading of target, $\{s_i\}_0$ and $\{s_i\}_1$ are the same, the WMR cannot differentiate one target from the other. Further, let $\Delta\theta_t$ be the error in the angle, and r_t be the target distance, $r_t\Delta\theta$ is the error of the arc length. As r_t increases, this arc length also increases as well. Hence, this grey

(error) area becomes larger as the target is farther away from the WMR. A nominal grid is selected for each area of the WMR working space for the total of 22 grids as shown in Fig. 1(b). To cope with these characteristics of the error, the model predictive control (MPC) is adopted in this work.

3. Formulation of Model Predictive Control Problem for RFID based WMR

3.1. Brief Summary on Model Predictive Control Technique

The MPC solution strategy in this study uses a moving 2-step predictive-window with the control applied over the first control window. In particular at a given time $t = t_k$, the problem is solved over $[t_k, t_{k+1}, t_{k+2}]$, where the WMR is supposed to reach the target at t_{k+2} as depicted in Fig. 2(b). The resulting control at the k^{th} iteration is applied only over $[t_k, t_{k+1}]$ to the WMR. After the control action takes place, the localization scheme is repeated to obtain the updated estimated position at t_{k+1}. The new control sequence is recomputed over $[t_{k+1}, t_{k+2}, t_{k+3}]$, and the process is repeated until the target is found, or other stopping criteria is met. Other number of windows can also be used. However, increasing the number of MPC window would result in higher computational cost.

3.2. Discrete State Equation for the RFID based WMR

For target tracking at the supervisory level, the state variables z_k are taken as the relative target position in the (x, y) coordinate, i.e., $z_k = [x_k^t, y_k^t]^T$,which can be expressed in the polar coordinate as $[x_k^t, y_k^t]^T = [r_k^t \cos(\theta_k^t), r_k^t \sin(\theta_k^t)]^T$. The control inputs are the travelling distance, and the heading angle of the WMR, i.e., $u = [u_r, u_\theta]^T$. When the control is applied, the WMR travels in the (x, y) coordinate, with respect to the WMR frame at time k, as

$$[x_{u,k}, y_{u,k}]^T = [u_{r,k} \cos(90^\circ - u_{\theta,k}),\ u_{r,k} \sin(90^\circ - u_{\theta,k})]^T \tag{2.1}$$

The new position (discrete state equation), $z_{k+1} = [x_{k+1}, y_{k+1}]^T$ is given by

$$x_{k+1} = r_k^t \cos(\theta_k^t) - u_{r,k}.\cos(90^\circ - u_{\theta,k})$$

$$y_{k+1} = r_k^t \sin(\theta_k^t) - u_{r,k}.\sin(90^\circ - u_{\theta,k}) \tag{2.2}$$

which can be rewritten in the polar form in eq. (2.3) and depicted in Fig. 2(a).

$$r_{k+1}^t = \sqrt{r_k^{t2} + {u_{r,k}}^2 - 2 r_k^t . u_{r,k} . \cos(\theta_k^t + u_{\theta,k} - 90^o)}$$

$$\theta_{k+1}^t = \tan^{-1}\left(\frac{r_k^t \sin(\theta_k^t) - u_{r,k}.\sin(90^\circ - u_{\theta,k})}{r_k^t \cos(\theta_k^t) - u_{r,k}.\cos(90^\circ - u_{\theta,k})} \right) \tag{2.3}$$

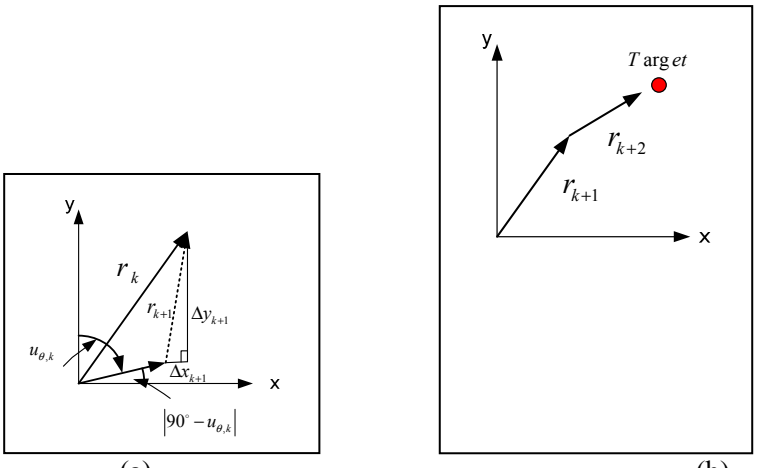

Fig. 2 (a) State transition from k to k+1; (b) 2-step control for WMR traveling to target at time k+2.

3.3. Performance Index Equation Section (Next)

The performance index (PI) is selected to reflect the desired behavior. Since the objective is to minimize the error of heading position and the distance from the target, PI is chosen as,

$$J = \sum_{j=k+1}^{k+2} w_{\theta,j} \left| \theta_{t,j} - 90^o \right| + \sum_{j=k+1}^{k+2} w_{r,j} \cdot r_{t,j} \tag{3.1}$$

where $\left| \theta_{t,j} - 90^o \right|$ is the heading error from 90 deg. at the j^{th} iteration; $r_{t,j}$ is the relative target position (from the WMR); $w_{\theta,j} \geq 0$, and $w_{r,j} \geq 0$ are the appropriate weighing coefficients. The objective of the WMR is to be within the vicinity of the target at the end of the 2nd control window $(k+2)$. Note that it is not desirable to exactly hit the target, i.e., $r_{t,k+2} = 0$, as the WMR can damage the target. In this study, the WMR stops when it arrives in the vicinity of the destination, which is set as $|r_t| < \varepsilon$. Hence, the modified PI is chosen as

$$J = \sum_{j=k+1}^{k+2} w_{\theta,j} \left| \theta_{t,j} - 90^o \right| + \sum_{j=k+1}^{k+2} w_{r,j} \cdot r_{t,j} \cdot (0.5 + 0.5 sgn(r_{t,j} - \varepsilon)) \tag{3.2}$$

The *sgn* function in equation (3.2) is chosen to penalize the WMR position outside the ε – radius circle centered at the target.

4. Simulation Results Equation Section (Next)

The threshold for stopping is $|r_t| < \varepsilon$, where $\varepsilon = 30$ cm. This boundary is shown as the circled dashed-line in Fig. 4. Since the target position at the end of the first window does not have to be extremely close to the target. The weight $w_{r,k+1} = 0$. This introduces the possibilities of singular solutions[1] to occur. Herein, the infinite number of solution results in the same cost. For example, let a target standing in front of the WMR, $\theta^t = 90^o$, while $u_{\theta,k}$ is kept at zero degree, any control sequence in equation (4.1) would result in zero-cost function. Due to the uncertainties during the location step, the estimated target position contains error, i.e., $r_k^t \in N_l(r^t)$, where $N_l(r^t)$ denotes the neighbourhood of r^t with the radius l. For the control choice in (4.1), the applied control has the travelling distance of $\alpha \cdot r_{t_k}$. The trajectories for the $\alpha = 0.3$, and 0.7 for the initial target of $(150,120)$ cm are shown in Fig. 3. The travelling time for both cases are 60 s. and 20 s., respectively. Higher number of steps for $\alpha = 0.3$ is obviously due to the shorter distance for the applied control. In another example, with initial target of (150,50) and $\alpha = 0.5$, the MPC can reach the target within 3 steps. However, the MPC with $\alpha = 0.7$ fails to stop when being in the vicinity of the target. As shown in Fig. 4(b), when the WMR is in the circle of the target, the angle is over 180°. Hence, with the aggressive setting, the robustness is compromised.

$$[u_{r,k}, u_{r,k+1}] = [\alpha \cdot r_{t_k}, (1-\alpha) r_{t_k}] \text{ for } \alpha \in [0,1] \tag{4.1}$$

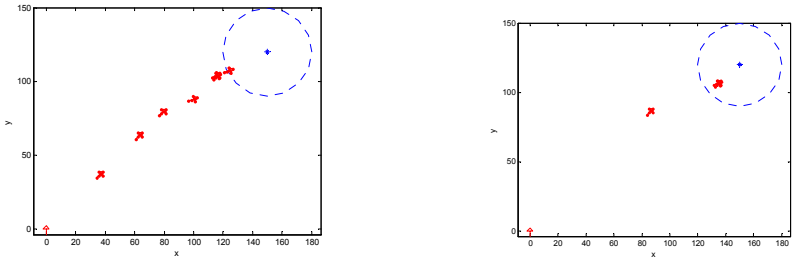

(a) (b)

Fig. 3 Trajectories for initial target of (150,120) with (a) $\alpha = 0.3$; (b) $\alpha = 0.7$

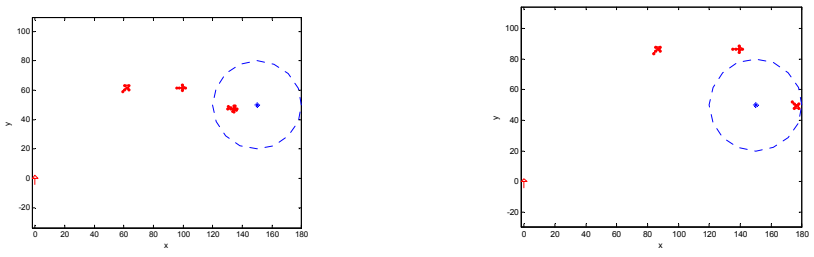

(a) (b)

[1] The Hamiltonians in the hybrid optimal control theory associated with this set of singular solutions are equal.

Fig. 4 Trajectories for initial target of (150,50) with (a) $\alpha = 0.5$; (b) $\alpha = 0.7$

5. Conclusions

The control of a single passive RFID based wheeled mobile robot (WMR) to reach the vicinity of the target was shown in this paper. The localization was based on the self-generated polar grids, where the estimation error decreased as the target distance decreased. The 2-step model predictive control was shown to be effective in dealing with the localization error, and other uncertainties. The trade-off between the target reaching time and the robustness was illustrated. With conservative setting for the MPC control, the WMR was more robust, and vice versa.

6. Acknowledgement

The experiment conducted in this work was supported by a research laboratory in the department of Electrical Engineering, Rajamangala University of Technology Lanna Chiang Rai.

7. References

[1] N. Pathanawongthum and P. Cherntanomwong, "RFID based localization techniques for indoor environment," in International Conference on Advanced Communication Technology, ICACT, 2010, pp. 1418-1421.

[2] S. Han, H. Lim, and J. Lee, "An efficient localization scheme for a differential-driving mobile robot based on RFID system," IEEE Transactions on Industrial Electronics, vol. 54, pp. 3362-3369, 2007.

[3] M. Kim and N. Y. Chong, "RFID-based mobile robot guidance to a stationary target," Mechatronics, vol. 17, pp. 217-229, 2007.

[4] S. Park and S. Hashimoto, "Autonomous mobile robot navigation using passive RFID in indoor environment," IEEE Transactions on Industrial Electronics, vol. 56, pp. 2366-2373, 2009.

[5] D. Boontrai, T. Jingwangsa, and P. Cherntanomwong, "Indoor localization technique using passive RFID tags," in 2009 9th International Symposium on Communications and Information Technology, ISCIT 2009, Icheon, 2009, pp. 922-926.

[6] W. Li, X. Jiang, and Y. Wang, "Road recognition for vision navigation of an autonomous vehicle by fuzzy reasoning," Fuzzy Sets and Systems, vol. 93, pp. 275-280, 1998.

[7] V. M. Peri and D. Simon, "Fuzzy logic control for an autonomous robot," in Annual Conference of the North American Fuzzy Information Processing Society - NAFIPS, Detroit, MI, 2005, pp. 337-342.

[8] D. E. Barkana, "Evaluation of low-level controllers for an orthopedic surgery robotic system," IEEE Transactions on Information Technology in Biomedicine, vol. 14, pp. 1128-1135, 2010.

[9] J. J. Zhan, C. H. Wu, and J. G. Juang, "Application of image process and distance computation to WMR obstacle avoidance and parking control," in Proceedings of the 2010 5th IEEE Conference on Industrial Electronics and Applications, ICIEA 2010, Taichung, 2010, pp. 1264-1269.

[10] S. Wei, M. Zefran, K. Uthaichana, and R. DeCarlo, "Hybrid model predictive control for stabilization of wheeled mobile robots subject to wheel slippage," in Proceedings of the IEEE International Conference on Robotics and Automation, Rome, 2007, pp. 2373-2378.

[11] J.-S. Kim, T.-W. Yoon, A. Jadbabaie, and C. De Persis, "Input-to-state stable finite horizon MPC for neutrally stable linear discrete-time systems with input constraints," Systems & Control Letters, vol. 55, pp. 293-303, 2006.

[12] J. Mattingley, W. Yang, and S. Boyd, "Receding Horizon Control," Control Systems, IEEE, vol. 31, pp. 52-65, 2011.

[13] K. Uthaichana, S. Bengea, R. DeCarlo, S. Pekarek, and M. Zefran, "Hybrid Optimal Theory and Predictive Control for Power Management in Hybrid Electric Vehicle," Journal of Nonlinear Systems and Applications, vol. 2, pp. 96-110, 2011.

[14] M. B. B. Sharifian, R.Rahnavard, and H.Delavari, "Velocity Control of DC Motor Based Intelligent methods and Optimal Integral State Feedback Controller," International Journal of Computer Theory and Engineering, vol. 1, pp. 81-84, 2009.